

## Nano-capacitors as batteries including graphene electrodes and Ga-N mixed with bio-polymers as insulator

Thu Thi Pham<sup>1</sup>, Majid Monajjemi<sup>1,2,\*</sup>, Dung My Thi Dang<sup>1</sup>, Fatemeh Mollaamin<sup>1</sup>, Chien Mau Dang<sup>1</sup>

<sup>1</sup>Institute for Nanotechnology (INT), Vietnam National University - Ho Chi Minh City (VNUHCM), Ho Chi Minh City, Vietnam

<sup>2</sup>Department of chemical engineering, Central Tehran Branch, Islamic Azad University, Tehran, Iran

\*corresponding author e-mail address: [Maj.monajjemi@iauctb.ac.ir](mailto:Maj.monajjemi@iauctb.ac.ir)

### ABSTRACT

Battery stores energy via a chemical process while a capacitor stores static electricity, therefore this generates when electric charges in a material are out of balance. Capacitors have several advantages than batteries because they charge and discharge faster, they don't use harmful chemicals, don't weigh as much and last longer. In this research, we have simulated one which is combined of a graphite layer that is separated through an insulating medium of polymerase's wurtzite Ga-N sheets. It has been shown that the alternate boron and nitrogen atoms instead of carbon are the suitable dopants for hetero-structures of the G// wurtzite Ga-N//G capacitors. We have shown that the Quantum effect has appeared in this capacitor due to the electropositive-electronegative coupled of wurtzite Ga-N and this effect cannot occur in the two electro negative or two electro positive elements layers. Therefore by this unique property our capacitor has been modeled to store a large capacity for green storage of energies in the new world of technologies.

**Keywords:** *graphene electrode, boron and nitrogen doping, nanoscale dielectric capacitors, wurtzite Ga-N dielectric.*

### 1. INTRODUCTION

Nanoscale capacitor has been developed for achieving the properties which are important to other systems of energy's storage and also they have been developed as one of the most significant energy storage mediums. Those capacitors are able to deliver higher quantities of charges at higher power limits. Their stable durability and quicker load periods select them beneficial in several subjects and equipment [1-5]. Recently; Graphene, h-BN, Ga-N and Nano capacitors including two electrodes and dielectric sheets have been developed in Nano biotechnology [5-7]. These nanoscale dielectric capacitors (NDC) consist of two metallic graphene layers separated through insulating N-Ga thin layer which has been applied for simulating in view point of structures and molecular designing. Experimentally and theoretically investigations on this system were focused for understanding the dielectric depended of these structures to form a unique capacitor including thin layers as charge holding mechanism [4-10]. Furthermore it was explained that graphene might be preserve current densities five order of magnitude larger than the silver [6-12]. Since the major goal of using capacitors are for reserving energies through storing equal magnitude of electrical charges in both opposite sign of two electrodes (plates), the charged capacitors are in a static and non-equilibrium state. The energies stored are liberated when the electrodes are connected together via an external circuit, so that the discharged mechanism shifts into an equilibrium state. In this study, we consider the above mentioned of NDC model including graphene as two electrodes which combined with Ga-N plates as insulator using ab initio, density functional theory (DFT) and Extended-Huckel calculations. This nanoscale capacitor model consists of a few hexagonal Ga-N layers, which are stacked between two graphene plates (Fig.1).

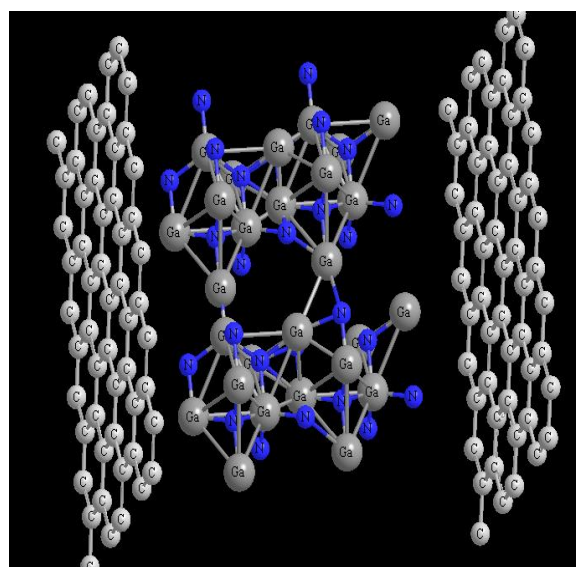


**Figure 1.** Nanoscale capacitor model consist of a wurtzite type Ga-N layer.

Gallium nitride (Ga-N) is a binary III/V direct bandgap. Semiconductor usually applied in light-emitting diodes since the 1990s. These compounds are very hard material which has a Wurtzite crystal structure. Its wide band gap of 3.4 eV cause several special properties for using in optoelectronic or high -power and frequencies instruments. As forinstance, Ga-N is the substrate which makes violet (405 nm) laser diodes possible, without the use of nonlinear optical frequency-doubling.

It is not sensitive to ionization with radiation therefore it is a suitable material for solar cell arrays for satellites and especially for militaries in spaces activities. Due to Ga-N transistors which operate at much higher temperatures and also work at much higher voltages is better material than gallium arsenide (GaAs) transistors.

Ga-N layer (Fig.2) has a suitable and wide band gap which can vail as an insulator dielectric material among the graphite layers. Since the distances between two electrodes and wall thickness of those insulators separation of these kind capacitors are less than 11 angstrom, the stored energy must be calculated from the first principles. In this work, the capacitance values have been obtained from the DFT and compared through an extended-Huckel method (QM/MM). Designing the spacing of capacitors between two electrode sheets at nanoscale is essential to achieve a high capacitance. So, the 3D combinations of those structures have been prepared via selected stacking of varying numbers of layers which can be enable us for offering number of options in constructing capacitors with different situations. Thus, in this kind capacitor model, considerable quantum size effects at small separations by varying the separation distances can be observed and must be evaluated.

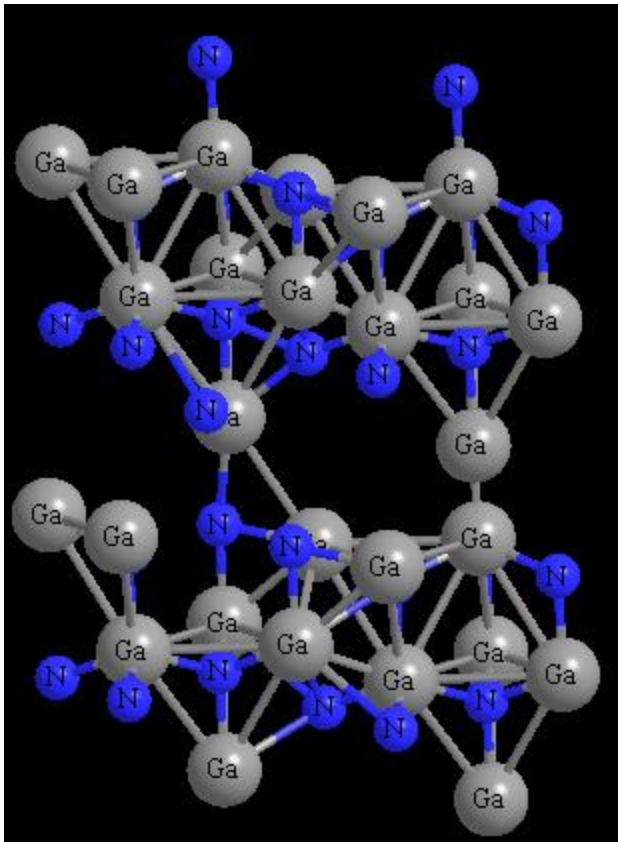


**Figure 2.** Ga-N layer has suitable and wide band gap.

In this investigation, a sample of a capacitor is made via creating a few insulating layers of (h-Ga-N) between two BN-doped graphene electrodes. It has been assumed that the electrodes field by  $\pm Q$  charges from one of the electrodes toward the opposite electrode. By letting the electrons tunnel via the insulating layers from the (-) to the (+) terminals, thus the charges ( $Q+\Delta q_e$ ) reside on the top sheet and ( $-Q -\Delta q_e$ ) resides on the bottom sheet of electrodes. Therefore the stored energies in this

## 2. MATERIALS AND METHODS

**Computational details:** Calculations were accomplished using Gaussian09 and GAMESS packages. In this investigation, it has been basically focused on the results from both DFT calculation

position are now  $E_f = \frac{(Q+\Delta q)^2}{2C}$  and the initial energies stored through an electrostatic field among the capacitor sheets and are given by equation  $E_i = \frac{Q^2}{2C}$ . These energies cannot be stored in the capacitor's sheets until an electron tunnels between insulator layers from the (-) to the (+) terminals.

Where the change in stored energy can be indicated as:  $\Delta E_s = E_f - E_i = \frac{\Delta q(Q+\frac{\Delta q}{2})}{C}$  (1). in this mechanism the larger voltages are in the range of  $-\frac{\Delta q}{2C} < \Delta V < +\frac{\Delta q}{2C}$ , which are the tunneling currents and will only flow during sufficient voltages  $|\Delta V| > |\frac{q_e}{2C}|$ . This effect is known as the coulomb blockade.

Obviously, the capacitor plate's separation, "d", might be small for the tunneling effect for any taking places in the system. In the macroscopic systems for a small capacitor (in the range of  $C \sim 10^{-13}$  F), it can be exhibited that amount of  $|\Delta V| > 1.6\mu V$  are needed for any tunneling occurring. And meanwhile for nanoscale capacitors with capacitances in the ranges of  $C \sim 10^{-17}$  F and so on, the amount of  $|\Delta V| > 1.6mV$  and for the nanoscale capacitor with  $C \sim 10^{-19}$  F, the range of  $|V| > 0.75$  are required for having the tunneling effects. Thus, coulomb block's effects are not appearing in the macro-sized circuits because of the low charging energies. However, it can be occur in the nanometers scales because of the charge quantization. For the small systems, the capacitances might be trivial that the charging energies " $\frac{e^2}{2C}$ ", is going to be great therefore the energy value for tunneling of the quantum position would then increase.

The tunneling resistances can also be assumed as:  $R_{Tun} = \frac{\Delta V}{I}$  (2) that are not a normal resistance, however, theoretically allowing electrons for crossing the insulating junction as discrete occurrences where "I" is the resulting current due to the tunneling effect. Tunneling resistance is an imaginary one which allows the electrons for crossing the insulating junction during " $t=R_{Tun}C_Q$ " (3) "and  $C_Q$  is the quantum capacitance. "t" is a time associated with tunneling events and is considered to be the approximate life-time for the energies states of each electron. The " $R_{Tun}$ ", have to be finite (not too big). Therefore in this condition, the charges are said to be well quantized and also the capacitors are evaluated to be a tunneling junction. When the quantum well descends below the Fermi's level, an electron start to be accommodated in the position of the quantum well and any further electrons (in the graphene layers) become sensitive for charging spilling into the vacuum spaces of the capacitors [12-27]. The hybrid capacitances and consequently the quantum capacitances are related to the net capacitances,  $C_{net}$ , via the equation of  $\frac{1}{C_{net}} = \frac{1}{C_g} + \frac{2}{C_Q}$  (4). It is notable that  $C_Q$  is many orders of magnitude greater than the  $C_g$ .

and extended Huckel. For ab-initio the m06, m06-L methods have been applied and Extended-Huckel has been used for the non-bonded interaction of G/ (Ga-N)/ G, which are monotonous

through the comparison between different situations. The m062x, m06-L, and m06-HF are a novel ultra-hybrid density functional including a good reference in non-bonded interactions and are suitable for calculating the energies of the distances among the fragments of the capacitors, in medium (~3–6Å), and long ranges of dielectric thickness (≥6 Å)[28-32]. The double ζ-basis sets including polarization orbitals have been applied for doped graphene atoms. Meanwhile, single ζ-basis sets with polarization orbitals have been employed for the Ga-N layers. For the non-covalent interactions, B<sub>3</sub>LYP and BLYP methods are unable for describing a van der Waals interaction between two plates of the capacitor system. In medium-range interaction, such as the interaction of two electrodes and also between dielectric and each electrode sheet meta- hybrid calculations are needed. In the lack of these kind abilities, most other popular functional describe medium-range of exchange and correlation energies limitation of their applicability for distant non-bonded systems between two electrodes and dielectric thickness. In addition, some recent works have been exhibited that in-accuracy for the medium-range exchange energies lead to large systematic errors for the prediction of molecular properties [33-36]. Geometry optimization and electronic structure evaluation have been carried out using the DFT approach which are based on an iterative solution of the Kohn-Sham equation of the density functional. The Perdew-Burke-Ernzerhof exchange correlation functional of the generalized gradient approximation (GGA) is adopted. In this simulation the two electrodes have doped through several percentages of boron atoms which are likely for adjusting to surrounding carbon host atoms. Therefore when graphene sheets are doped with one boron atom, this atom also undergoes sp<sup>2</sup> hybridization. Because of the nearly same size of C and B, no significant distortions in 2-D structure of graphene are expected, except for changing in adjoining bond length. As a result, the bond lengths are found for expanding to 1.48 Å. Using the computational procedure as mentioned, the electronic properties and band structures are possible to be calculated.

The electron densities have been defined as  $\rho(r) = \eta_i |\varphi_i(r)|^2 = \sum_i \eta_i |\sum_l C_{li} \chi_l(r)|^2$  (5). [39] Where  $\eta_i$  is orbital (*i*),  $\varphi$  are orbital

### 3. RESULTS

In this investigation, Ga-N was selected as a capacitor sheet since it is suitable electrodes with excellent lattice constant near to that point of graphene. We specifically investigated the dielectric properties of graphene // (Ga-N)<sub>m</sub> // graphene, stacking for m= 1, 2 and 3 layers of dielectrics. The results are plotted in 6 Figures and the data are placed in two tables. Since the “BN” in nature is an ideal electrical chemical bond that can be polarized by applying an external electric field, the number of Ga-N between two plates of graphene has been calculated and optimized as a suitable simulation of dielectrics Table.1 and Figs 1-6.

Furthermore, graphene is well-known single layer honeycomb structure, so the proposed model can be easily fabricated. Similar to graphene, the anisotropic binding of G-BN allows for the formation of several layered structures. Long-range

wave functions,  $\chi$  are basis functions. Atomic unit for electron density can be explicitly written as  $e/\text{Bohr}^3$ .  $\nabla\rho(r) = [(\frac{\partial\rho(r)}{\partial(x)})^2 + (\frac{\partial\rho(r)}{\partial(y)})^2 + (\frac{\partial\rho(r)}{\partial(z)})^2]^{\frac{1}{2}}$  (6)  $\nabla^2\rho(r) = \frac{\partial^2\rho(r)}{\partial x^2} + \frac{\partial^2\rho(r)}{\partial y^2} + \frac{\partial^2\rho(r)}{\partial z^2}$  (7) [39].

Through doping B atoms in graphite Fermi level shifts significantly below the Dirac point resulting into a p-type doping. Therefore symmetry of graphite breaks into two graphene sublattices. The charge transfer and electrostatic potential-derived charge were also calculated using the Merz-Kollman-Singh, chelp, or chelpG which a detailed overview of this effect the charge distribution can be calculated. Although infinite graphite sheets are intrinsically metallic, our works indicate an increase in the metallic properties. The interaction energy for capacitor was calculated in all items as indicated in equation 9:  $\Delta E_S(eV) = \{E_C - (2E_G + E_{GaN})\} + E_{BSSE}$  (8) where the “ $\Delta E_S$ ” is the stability energy of capacitor. Based on some previous work our calculation has been modeled and simulated [40-67].

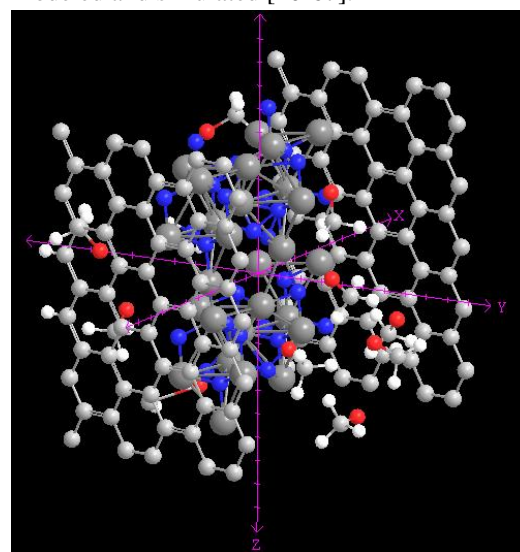


Figure 3. Nanoscale capacitor model consist of a wurtzite type Ga-N layer inside polymer' solvent.

interlayer's interactions plays suitable dominant in characterizing the structural and mechanical properties of those systems.

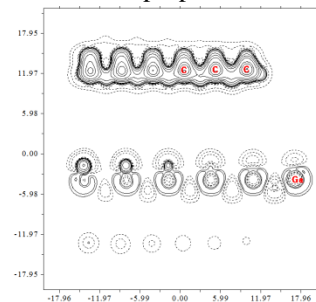


Figure 4. The situation of Kinetic Energy of Ga-N as G/ Ga-N/G capacitor

The values of the distances between Ga-N layers capping graphene layers, dielectric constants of the layered sheets (*k*),

magnitude of the charges on the graphene plates, electrostatic properties using the SCF density, fitting point charges to electrostatic potential charges from ESP fit, the stability energy of capacitor (eV), various capacitances including the net capacitance and the potential difference between two electrodes of graphene plates are listed in Tables 1 & 2. Different numbers of dopants indicate proper situations for boron dopants in graphene electrodes. The potential energy difference between the two electrode layers,  $V = \Delta_{EP} = \sum_{i=1}^{46} (EP_{GaNG_1} - EP_{GaNG_2})$  (a.u.) are depicted in table 2 and varies between 2.45 and 4.20 volts (Table 2), which leads to the accumulation of approximately identical amount of surface charges of the opposite sign.

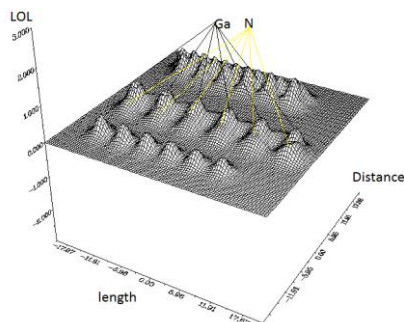


Figure 5. The situation of Density Energy of Ga-N as G/ Ga-N/G capacitor versus X, Y and Z-axis in Bohr.

Here we have considered the interlayer attraction using Extended-Huckel force field for G-BN to describe its interlayer interactions including wurtzite -Ga-N inter-layer potential, attractive components and the classical mono-polar electrostatic term that takes into account the partially ionic character of h-Ga-N (Fig. 4).

In this study, the number of h-Ga-N layers as a dielectric is 1, 2 and 3. For the nanoscale G/ (Ga-N)<sub>m</sub>/ G and planar capacitor, the different voltages can be estimated from the band gap. For long distances of dielectric thickness, the classical capacitance rule of the “ $C_g \propto \frac{1}{d}$ ” is adaptable. This adaptability does not go for short distances, which is attributed to the quantum size effect. We identified the dielectric permittivity as a function of dielectric size through ab-initio calculations Fig. 5.

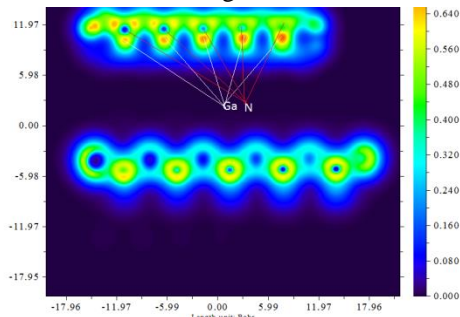


Figure 6. The color counter map of LOL Energies of Ga-N as G/ Ga-N/G capacitor

Table 2. The potential energy difference of modeled capacitors in various thicknesses

“Nano capacitor” Various sequence	Number of insulator layers	$\Delta V = \sum_{i=1}^{46} (EP_{G_1} - EP_{G_2})$
	m	A B C
G/ (GaN)/G	1	2.453.10 2.70
G/ (GaN)2/G	2	3.103.904.20
G/ (GaN)3/G	3	3.252.152.30

Table 1. The Charges of two G/ (GaN)/G and the stability energies.

“Nano capacitor” Various sequence	Number of insulator layers	$\frac{1}{2}$ Dielectric of thickness $A = d_1 B = d_2 C = d_3$	$\Delta E_5$ (eV)			$ \Delta q  = \sum_{i=1}^{46} (q_{G_1} - q_{G_2})$		
			A	B	C	A	B	C
G/ (GaN)/G	1	7.158.35 6.78	0.240.310.88			0.58	0.450.46	
G/ (GaN)2/G	2	9.65 9.50 11.15	0.32 0.58 1.75			1.24	1.26 1.25	
G/ (GaN)3/G	3	12.45 13.10 13.15	1.721.631.98			0.650.440.35		

#### 4. CONCLUSIONS

In this study, we have shown the model of a nanoscale dielectric capacitor composed of a few dopant including metallic graphene layers separated by an insulating medium containing a

few wurtzite -Ga-N layers. The capacitor with one layers of wurtzite -Ga-N has a high dielectric constant compared to other layers of wurtzite -Ga-N.

#### 5. REFERENCES

1. Yang, Z.G.; Zhang, J.-L.; Kintner-Meyer, M.C.W.; Lu, X.C.; Choi, D.W.; Lemmon, J.P.; Liu, J. Electrochemical energy storage for green grid. *Chem. Rev.* **2011**, *111*, 3577–3613, <https://doi.org/10.1021/cr100290v>
2. Guerard, D.; Herold, A. Intercalation of lithium on to Graphene and other carbons. *Carbon* **1975**, *13*, 337-345, [https://doi.org/10.1016/0008-6223\(75\)90040-8](https://doi.org/10.1016/0008-6223(75)90040-8).
3. Yoo E.J, Kim J., Hosono E., Zhou H.S., Kudo T., Large reversible Li storage of graphene nano-sheet families for use in rechargeable lithium ion batteries. *Nano. Lett* **2008**, *8*, 2277-2282, <https://doi.org/10.1021/nl800957b>.
4. Wang, G.; Shen, X.P.; Yao, J.; Park, J. Graphene nano-sheets for enhanced lithium storage in lithium ion batteries. *Carbon* **2009**, *47*, 2049-2053, <https://doi.org/10.1016/j.carbon.2009.03.053>

5. Bhardwaj, T.; Antic, A.; Pavan, B.; Barone, V.; Fahiman, B.D. Enhanced electrochemical lithium storage by graphene nano-ribbons. *J. Amer. Chem. Soc.* **2010**, *132*, 12556-12558
6. Suzuki, T.; Hasegawa, T.; Mukai, S.R.; Tamon, H.A. theoretical study on storage states of Li ions in carbon anodes of Li ion batteries using molecular orbital calculations. *Carbon* **2003**, *41*, 1933-1939
7. Monajjemi, M. Non-covalent attraction of B2N (-,0) and repulsion of B2N(+) in the BnNn ring: a quantum rotatory due to an external field. *Theoretical chemistry accounts* **2015**, *134*, 1-22, <https://doi.org/10.1007/s00214-015-1668-9>.
8. Noel, M.; Suryanarayanan, V. Role of carbon host lattices in Li-ion intercalation/de-intercalation processes. *Journal of Power Sources* **2002**, *111*, 193–209, [https://doi.org/10.1016/S0378-7753\(02\)00308-7](https://doi.org/10.1016/S0378-7753(02)00308-7).

9. Tirado, J.L. Inorganic materials for the negative electrode of lithium-ion batteries: state-of-the-art and future prospects. *Materials Science and Engineering R* **2003**, *40*, 103–136, [https://doi.org/10.1016/S0927-796X\(02\)00125-0](https://doi.org/10.1016/S0927-796X(02)00125-0).
10. Fu, L.J.; Liu, H.; Li, C.; Wu, Y.P.; Rahm, E.; Holze, R.; Wu, H.Q. Surface modifications of electrode materials for lithium ion batteries. *Solid State Sciences* **2006**, *8*, 113–128, <https://doi.org/10.1016/j.solidstatesciences.2005.10.019>.
11. Frackowiak, E.; Béguin, F. Electrochemical storage of energy in carbon nanotubes. *Carbon* **2002**, *40*, 1775–1787, [https://doi.org/10.1016/S0008-6223\(02\)00045-3](https://doi.org/10.1016/S0008-6223(02)00045-3).
12. Monajjemi, M. Non bonded interaction between BnNn (stator) and BN(-,0,+)B (rotor) systems: A quantum rotation in IR region. *Chemical Physics* **2013**, *425*, 29–45, <https://doi.org/10.1016/j.chemphys.2013.07.014>.
13. Safran, S.A.; Hamann, D.R. Long-Range Elastic Interactions and Staging in Graphite Intercalation Compounds. *Physical Review Letters* **1979**, *42*, 1410–1413, <https://doi.org/10.1103/PhysRevLett.42.1410>.
14. Monajjemi, M.; Chegini, H.; Mollaamin, F.; Farahani, P. Theoretical Studies of Solvent Effect on Normal Mode Analysis and Thermodynamic Properties of Zigzag (5,0) carbon nanotube. *Fullerens Nanotubes carbon and nanostructures* **2011**, *19*, 469–482, <https://doi.org/10.1080/1536383X.2010.494783>.
15. Levy, P.M.; Morin, P.; Schmitt, D. Large Quadrupolar Interactions in Rare-Earth Compounds. *Phys. Rev. Lett.* **1979**, *42*, 1417, <https://doi.org/10.1103/PhysRevLett.42.1417>.
16. Monajjemi, M.; Baei, M.T.; Mollaamin, F. Quantum mechanics study of hydrogen chemisorptions on nanocluster vanadium surface, *Russian journal of inorganic chemistry* **2008**, *53*, 1430–1437, <https://doi.org/10.1134/S0036023608090143>.
17. Lee, J.K.; An, K.W.; Ju, J.B.; Cho, B.W.; Cho, W.I.; Park, D.; Yun, K.S. Electrochemical Properties of Pan-Based Carbon Fibers as Anodes for Rechargeable Lithium Ion Batteries. *Carbon* **2001**, *39*, 1299–1305, [https://doi.org/10.1016/S0008-6223\(00\)00237-2](https://doi.org/10.1016/S0008-6223(00)00237-2).
18. Ehrlich, G.M. In: *Handbook of Batteries*, 3rd ed., David Linden, (Ed.), McGrawHill, 2002, pp. 35.16–35.21.
19. Churikov, A.V.; Gridina, N.A.; Churikova, N.V. New Carbon Based Materials for Electrochemical Energy Storage Systems. *Springer* **2006**, 269–276, <https://doi.org/10.1007/1-4020-4812-2>.
20. Naoi, K.; Ogihara, N.; Igarashi, Y.; Kamakura, A.; Kusachi, Y.; Utsugi, K. New Materials and New Configurations for Advanced Electrochemical Capacitors. *Journal of the Electrochemical Society* **2005**, *152*, A1047–A1053.
21. Monajjemi M., Faham R., Mollaamin F., Ab initio Study of Direct Diffusion Pathway for H<sup>+</sup>, Li<sup>+</sup>, Na<sup>+</sup>, K<sup>+</sup> Cations into the (3,3), (4,4), and (5,5) Open-Ended Single-Walled Carbon Nanotubes. *Fullerens Nanotubes carbon and carbon nanostructures* **2012**, *20*, 163–169.
22. Endo, M.; Nishimura, Y.; Takahashi, T.; Takeuchi, K. Dresselhaus M.S., Lithium storage behavior for various kinds of carbon anodes in Li ion secondary battery. *Journal of Physics and Chemistry of Solids* **1996**, *57*, 725–728, [https://doi.org/10.1016/0022-3697\(95\)00339-8](https://doi.org/10.1016/0022-3697(95)00339-8).
23. Chandrashekar, S.; Nicole, M.; Chang, H.J.; Du, L.S.; Grey, C.P.; Jerschow, A. Li MRI of Li batteries reveals location of microstructural lithium. *Nature Materials* **2012**, *11*, 311–315, <https://doi.org/10.1038/nmat3246>.
24. Yang, Z.H.; Wu, H.Q. Electrochemical interaction of lithium into raw carbon nanotubes. *Mater. Chem. Phys.* **2001**, *71*, 7–11.
25. [25] Wilkinson D.S., Mass Transport in Solid and Fluids. *Cambridge University Press* **2000**, <https://doi.org/10.1017/CBO9781139171267>.
26. Mehrer, H. *Diffusion in Solids*, Springer 2007, pp. 27–36, <https://doi.org/10.1007/978-3-540-71488-0>.
27. Porter, D.A.; Easterling, K.E. *Phase Transformations in Metals and Alloys*, 2nd ed.; Chapman & Hall, 1992, pp. 1–109.
28. Mollaamin, F.; Najafpour, J.; Ghadami, S.; Akrami, M.S.; Monajjemi, M. The Electromagnetic Feature of B15N15Hx (x=0, 4, 8, 12, 16, and 20) Nano Rings: Quantum Theory of Atoms in Molecules/NMR Approach. *Journal of computational and theoretical nanoscience* **2014**, *11*, 1290–1298.
29. Monajjemi, M.; Ahmadianarog, M. Carbon Nanotube as a Deliver for Sulforaphane in Broccoli Vegetable in Point of Nuclear Magnetic Resonance and Natural Bond Orbital Specifications. *Journal of computational and theoretical nanoscience* **2014**, *11*, 1465–1471.
30. Lee, V.S.; Nimmanpipug, P.; Mollaamin, F.; Kungwan, N.; Thanasanvorakun, S.; Monajjemi, M. Investigation of single wall carbon nanotubes electrical properties and normal mode analysis: Dielectric effects. *Russian journal of physical chemistry A* **2009**, *83*, 2288–2296, <https://doi.org/10.1134/S0036024409130184>.
31. Monajjemi M., Mahdavian L., Mollaamin F., Characterization of nanocrystalline silicon germanium film and nanotube in adsorption gas by monte carlo and langevin dynamic simulation, *Bulletin of the chemical society of Ethiopia* **2008**, *22*, 277–286, <http://dx.doi.org/10.4314/bcse.v22i2.61299>.
32. Monajjemi, M.; Ghiasi, R.; Ketabi, S.; Pasdar, H.; Mollamin, F. A theoretical study of metal-stabilised rare tautomers stability: N4 metalated cytosine (M=Be<sup>2+</sup>, Mg<sup>2+</sup>, Ca<sup>2+</sup>, Sr<sup>2+</sup> and Ba<sup>2+</sup>) in gas phase and different solvents, *Journal of chemical research* **2004**, *1*, 11–18, <https://doi.org/10.3184/030823404323000648>.
33. Monajjemi, M.; Ghiasi, R.; Sadjadi, M.A.S. Metal-stabilized rare tautomers: N4 metalated cytosine (M = Li<sup>+</sup>, Na<sup>+</sup>, K<sup>+</sup>, Rb<sup>+</sup> and Cs<sup>+</sup>), theoretical views, *Applied organometallic chemistry* **2003**, *17*, 635–640, <https://doi.org/10.1002/aoc.469>.
34. Monajjemi, M.; Mahdavian, L.; Mollaamin, F.; Honarparvar, B. Thermodynamic Investigation of EnolKeto Tautomerism for Alcohol Sensors Based on Carbon Nanotubes as Chemical Sensors. *Fullerens nanotubes and carbon nanostructures* **2010**, *18*, 45–55, <https://doi.org/10.1080/15363830903291564>.
35. Hadad, B.K.; Mollaamin, F.; Monajjemi, M. Biophysical chemistry of macrocycles for drug delivery: a theoretical study. *Russian chemical bulletin* **2011**, *60*, 238–241, <https://doi.org/10.1007/s11172-011-0039-5>.
36. Monajjemi, M.; Honarparvar, B.; Hadad, B.K.; Ilkhani, A.R.; Mollaamin F. Thermo-chemical investigation and NBO analysis of some anxiolytic as Nano- drugs. *African journal of pharmacy and pharmacology* **2010**, *4*, 521–529.
37. Monajjemi, M.; Naderi, F.; Mollaamin, F.; Khaleghian, M. Drug Design Outlook by Calculation of Second Virial Coefficient as a Nano Study. *Journal of the mexican chemical society* **2012**, *56*, 207–211.
38. Ilkhani, A.R.; Monajjemi, M. The pseudo Jahn-Teller effect of puckering in pentatomic unsaturated rings C(4)AE(5), A = N, P, As, E = H, F, Cl. *Computational and theoretical chemistry* **2015**, *1074*, 19–25.
39. Lu, T.; Chen, F. Multiwfn: A Multifunctional Wavefunction Analyzer. *J. Comp. Chem.* **2012**, *33*, 580–592, <https://doi.org/10.1002/jcc.22885>.
40. Monajjemi, M.; Mohammadian, N.T.S-NICS an Aromaticity Criterion for Nano Molecules. *J. Comput. Theor. Nanosci* **2015**, *12*, 4895–4914, <https://doi.org/10.1166/jctn.2015.4458>.

41. Monajjemi, M.; Lee, V.S.; Khaleghian, M.; Honarparvar, B.; Mollaamin, F. Theoretical Description of Electromagnetic Nonbonded Interactions of Radical, Cationic, and Anionic NH<sub>2</sub>BHNBNH<sub>2</sub> Inside of the B18N18 Nanoring. *J. Phys. Chem C* **2010**, *114*, 15315, <https://doi.org/10.1021/jp104274z>.
42. Monajjemi, M.; Boggs, J.E. A New Generation of BnNn Rings as a Supplement to Boron Nitride Tubes and Cages. *J. Phys. Chem. A* **2013**, *117*, 1670–1684, <https://doi.org/10.1021/jp312073q>.
43. Monajjemi, M.; Robert, W.J.; Boggs, J.E. NMR contour maps as a new parameter of carboxyl's OH groups in amino acids recognition: A reason of tRNA–amino acid conjugation, *Chemical Physics* **2014**, *433*, 1–11, <https://doi.org/10.1016/j.chemphys.2014.01.017>.
44. Monajjemi, M. Quantum investigation of non-bonded interaction between the B15N15 ring and BH<sub>2</sub>NBH<sub>2</sub> (radical, cation, and anion) systems: a nano molecular motor. *Struct Chem* **2012**, *23*, 551–580, <https://doi.org/10.1007/s11224-011-9895-8>.
45. Monajjemi, M. Non-covalent attraction of B<sub>2</sub>N (2, 0) and repulsion of B<sub>2</sub>N (+) in the BnNn ring: a quantum rotatory due to an external field. *Theor Chem Acc* **2015**, *134*, 1668–9, <https://doi.org/10.1007/s00214-015-1668-9>.
46. Monajjemi, M. Metal-doped graphene layers composed with boron nitride–graphene as an insulator: a nano-capacitor. *Journal of Molecular Modeling* **2014**, *20*, 2507, <https://doi.org/10.1007/s00894-014-2507-y>.
47. Monajjemi, M.; Najafpour, J. Charge density discrepancy between NBO and QTAIM in single-wall armchair carbon nanotubes. *Fullerenes Nanotubes and Carbon Nanostructures* **2014**, *22*, 575–594, <https://doi.org/10.1080/1536383X.2012.702161>.
48. Mollaamin, F.; Monajjemi, M. DFT outlook of solvent effect on function of nano bioorganic drugs. *Physics and Chemistry of Liquids* **2012**, *50*, 596–604, <https://doi.org/10.1080/00319104.2011.646444>.
49. Monajjemi, M. Cell membrane causes the lipid bilayers to behave as variable capacitors: A resonance with self-induction of helical proteins. *Biophysical Chemistry* **2015**, *207*, 114–127, <https://doi.org/10.1016/j.bpc.2015.10.003>.
50. Monajjemi, M.; Mahdavian, L.; Mollaamin, F. Interaction of Na, Mg, Al, Si with carbon nanotube (CNT): NMR and IR study. *Russian Journal of Inorganic Chemistry* **2009**, *54*, 9, 1465–1473, <https://doi.org/10.1134/S0036023609090216>.
51. Monajjemi, M. Liquid-phase exfoliation (LPE) of graphite towards graphene: An ab initio study. *Journal of Molecular Liquids* **2017**, *230*, 461–472, <https://doi.org/10.1016/j.molliq.2017.01.044>.
52. Monajjemi, M. Study of CD<sup>5+</sup> Ions and Deuterated Variants (CH<sub>x</sub>D<sub>(5-x)<sup>+</sup></sub>): An Artefactual Rotation. *Russian Journal of Physical Chemistry a* **2018**, *92*, 2215–2226.
53. Alemi-Tameh, F.; Safaei-Ghomi, J.; Mahmoudi-Hashemi, M.; Monajjemi, M. Amino Functionalized Nano Fe<sub>3</sub>O<sub>4</sub>@SiO<sub>2</sub> as a Magnetically Green Catalyst for the One-Pot Synthesis of Spirooxindoles Under Mild Conditions. *Polycyclic Aromatic* **2018**, *38*, 199–212, <https://doi.org/10.1080/10406638.2016.1179650>.
54. Elsagh, A.; Zare, K.; Monajjemi, M. Calculation of the magnetic resonance isotropy tensors of the nucleus of POPC phospholipid bilayers in a cell membrane. *Ukrainian Journal of Ecology* **2018**, *8*, 1, 165–173, [http://dx.doi.org/10.15421/2018\\_202](http://dx.doi.org/10.15421/2018_202).
55. Zakeri, M.; Monajjemi, M. Effective molecules of some natural product as antidepressant and antihistamine drugs: A NMR study. *Ukrainian Journal of Ecology* **2018**, *8*, 255–262.
56. Bagheri, S.; Aghaei, H.; Monajjemi, M. Novel Au-Fe<sub>3</sub>O<sub>4</sub> NPs Loaded on Activated Carbon as a Green and High Efficient Adsorbent for Removal of Dyes from Aqueous Solutions: Application of Ultrasound Wave and Optimization. *Eurasian Journal of Analytical Chemistry* **2018**, *13*, 3, <https://doi.org/10.29333/ejac/81809>.
57. Moosavi, M.S.; Monajjemi, M.; Zare, K. A Nano Catalyst of CoFe<sub>2</sub>O<sub>4</sub>@B18N18 as A Novel Material. *Oriental Journal of Chemistry* **2017**, *33*, 1648, <http://dx.doi.org/10.13005/ojc/330408>.
58. Monajjemi, M. Graphene/(h-BN)(n)/X-Doped Graphene As Anode Material in Lithium Ion Batteries. *Macedonian Journal of Chemistry and Chemical Engineering* **2017**, *36*, 101–118, <http://dx.doi.org/10.20450/mjcc.2017.1134>.
59. Farhami, N.; Monajjemi, M.; Zare, K. Non Bonded Interactions in cylindrical capacitor of (m, n) @ (m', n') @ (m'', n'') Three Walled Nano Carbon Nanotubes. *Oriental Journal of Chemistry* **2017**, *33*, 3024–3030, <http://dx.doi.org/10.13005/ojc/330640>.
60. Madani, M.S.; Monajjemi, M.; Aghaei, H. The Double Wall Boron Nitride Nanotube: Nano-Cylindrical Capacitor, *Oriental Journal of Chemistry* **2017**, *33*, 1213–1222, <http://dx.doi.org/10.13005/ojc/330320>.
61. Shahriari, S.; Monajjemi, M.; Zare, K. Increasing the efficiency of some antibiotics on penetrating bacteria cell membrane. *Ukrainian Journal of Ecology* **2018**, *8*, 671–679, [http://dx.doi.org/10.15421/2018\\_265](http://dx.doi.org/10.15421/2018_265).
62. Ryu, H.Y. Evaluation of Light Extraction Efficiency of GaN-Based Nanorod Light-Emitting Diodes by Averaging over Source Positions and Polarizations. *Crystals* **2018**, *8*, 27, <https://doi.org/10.3390/cryst8010027>.
63. Ding, K.; Avrutin, V.; Özgür, Ü.; Morkoç, H. Status of Growth of Group III-Nitride Heterostructures for Deep Ultraviolet Light-Emitting Diodes. *Crystals* **2017**, *7*, 300, <https://doi.org/10.20944/preprints201709.0013.v1>.
64. Wu, C.C.; Jeng, S.-L. Simulation Model Development for Packaged Cascode Gallium Nitride Field-Effect Transistors. *Crystals* **2017**, *7*, 250, <https://doi.org/10.3390/cryst7080250>.
65. Yuan, S.H.; Chang, F.Y.; Wu, D.S.; Horng, R.H. AlGaIn/GaN MOS-HEMTs with Corona-Discharge Plasma Treatment. *Crystals* **2017**, *7*, 146, <https://doi.org/10.3390/cryst7050146>.
66. Lin, P.J.; Tien, C.H.; Wang, T.Y.; Chen, C.L.; Ou, S.L.; Chung, B.C.; Wu, D.S. On the Role of AlN Insertion Layer in Stress Control of GaN on 150-mm Si (111) Substrate. *Crystals* **2017**, *7*, 134, <https://doi.org/10.3390/cryst7050134>.
67. Kishimoto, K.; Funato, M.; Kawakami, Y. Effects of Al and N<sub>2</sub> Flow Sequences on the Interface Formation of Al-N on Sapphire by EVPE. *Crystals* **2017**, *7*, 123,

## 6. ACKNOWLEDGEMENTS

This research is supported by Vietnam National University – Ho Chi Minh City (VNU-HCM) under the grant number TX2018-32-01.



© 2019 by the authors. This article is an open access article distributed under the terms and conditions of the Creative Commons Attribution (CC BY) license (<http://creativecommons.org/licenses/by/4.0/>).